Li+ solvation in ethylene carbonate–propylene carbonate concentrated solutions: A comprehensive model

ARTICLE *in* THE JOURNAL OF CHEMICAL PHYSICS · OCTOBER 1997

Impact Factor: 2.95 · DOI: 10.1063/1.474334

5 AUTHORS, INCLUDING:

Enzo Cazzanelli
Università della Calabria
133 PUBLICATIONS **1,443** CITATIONS
SEE PROFILE

Fausto Croce
Università degli Studi G. d'Annunzio Chieti e …
167 PUBLICATIONS **6,191** CITATIONS
SEE PROFILE

Giovanni B Appetecchi
ENEA
164 PUBLICATIONS **4,771** CITATIONS
SEE PROFILE

P. Mustarelli
University of Pavia
36 PUBLICATIONS **571** CITATIONS
SEE PROFILE

Li+ solvation in ethylene carbonate–propylene carbonate concentrated solutions: A comprehensive model

E. Cazzanelli, Fausto Croce, Giovanni Battista Appetecchi, Francesca Benevelli, and Piercarlo Mustarelli

Citation: J. Chem. Phys. **107**, 5740 (1997); doi: 10.1063/1.474334
View online: http://dx.doi.org/10.1063/1.474334
View Table of Contents: http://jcp.aip.org/resource/1/JCPSA6/v107/i15
Published by the American Institute of Physics.

Li^+ solvation in ethylene carbonate–propylene carbonate concentrated solutions: A comprehensive model

E. Cazzanelli
Department of Physics, University of Calabria and INFM, 87036 Cosenza, Italy

Fausto Croce and Giovanni Battista Appetecchi
Department of Chemistry, University ''La Sapienza,'' 00185 Roma, Italy

Francesca Benevelli
Centro Grandi Strumenti of University of Pavia, Via Bassi 21, 27100 Pavia, Italy

Piercarlo Mustarelli[a)]
CSTE-CNR and Department of Physical Chemistry of University of Pavia, Via Taramelli 16, 27100 Pavia, Italy

(Received 6 May 1997; accepted 26 June 1997)

Spectroscopic (Raman, NMR, impedance spectroscopy), and thermal [differential scanning calorimetry (DSC)] techniques have been used to study the solvation mechanism of lithium ions in ethylene carbonate (EC)–propylene carbonate (PC) concentrated solutions. For values of $N=[Li^+]/[EC+PC]\leqslant 0.2$ all the cations are solvated by ~ 4 solvent molecules and interaction chiefly takes place between Li^+ and the ring oxygens. For $N>0.2$ a part of Li^+ ions begins to form complexes with two solvent molecules (sandwich configuration). At $N\cong 0.5$ nearly all cations are complexed, and a crystalline compound is formed at room temperature. For higher values of N a reassociation of the salt takes place. © *1997 American Institute of Physics.* [S0021-9606(97)50937-8]

I. INTRODUCTION

Both aqueous and nonaqueous diluted solutions have been studied for a long time as model systems to verify the validity of classical electrodynamics.[1] The level of knowledge attained in this field allowed the definition of good microscopic models both for salt solvation and the transport properties.[2,3] In this concentration range (up to 10^{-3} M) the bulk of information was obtained by conductometric measurements and dielectric relaxation spectroscopy.[4] Recently, the results obtained by these conventional techniques have been confirmed using other spectroscopies like Raman, infrared (IR), far IR, and nuclear magnetic resonance (NMR).[5–8]

The development of more sophisticated diffractometric techniques like radial distribution function (RDF) allowed us to extend the range of investigations up to concentrations reaching 1–2 M, where the conductometric approach is ineffective due to the strong interactions among ions and between ions and dipoles. However, the structural information given by this approach is statistically mediated over a ''long'' time. In addition, RDF is not effective in the case of lithium as the cation.

The knowledge of structure and dynamics in highly concentrated solutions is becoming more and more important because of the applicability of these systems in the field of advanced electrochemical devices.[9] In fact, the operating conditions of electrochemical devices may cause the electrolyte to locally reach salt concentrations much higher that the nominal one. For example, a common phenomenon experienced in lithium batteries is the solvent degradation at the metallic lithium surface, which in certain cases can lead to the precipitation of the salt.[10]

We have undertaken a detailed work to investigate both structure and dynamics of Li^+ ions in highly concentrated solutions $LiClO_4$–EC–PC. We have tested solutions with a fixed EC/PC molar ratio (2.447) and $LiClO_4$ concentration increasing up to saturation limit. The study has been performed using a number of techniques, namely, impedance spectroscopy (IS), IR, and Raman spectroscopy, NMR, thermal analysis, viscosity measurements. In a previous paper we showed with ^{13}C NMR and Raman spectroscopy that some relevant modifications occur for a molar ratio $N=[Li^+]/[EC+PC]\cong 0.5$.[11] At this concentration, we postulated that nearly all the lithium ions are sandwiched between two solvent molecules without any selectivity (see Fig. 1). For greater values of N a reassociation takes place between Li^+ and ClO_4^-.

In another paper[12] we discussed conductivity and thermal data. At the critical concentration, $N\cong 0.5$, the conductivity no longer follows the usual Vogel–Tamman–Fulcher[13] behavior, but displays an anomaly near 40 °C, where an endotherm (assigned to the melting of a crystalline phase) is observed by DSC. Below this temperature the conductivity is best-fitted by the Arrhenius law.

In this paper we present a detailed and quantitative Raman study corroborated by ^7Li NMR data on $LiClO_4$/EC/PC solutions in a wide range of concentrations ($0.069\leqslant N\leqslant 1.01$). Particular attention is devoted to the concentrations around the ''critical'' values that show anomalies in the conductivity behavior. By comparing the spectroscopic data with both conductivity and differential scanning calorimetry

a)Author to whom correspondence should be addressed.

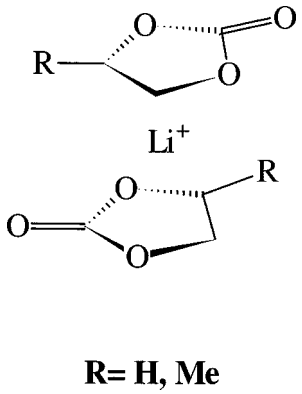

FIG. 1. ''Sandwich''-type coordination of the lithium ions (see text).

(DSC) measurements we discuss a sort of ''phase diagram'' of the pseudobinary system $LiClO_4$:(EC+PC). To our knowledge, this is the first comprehensive study on the Li^+ solvation in highly concentrated solutions of nonaqueous, ring-based organic solvents.

II. EXPERIMENT

$LiClO_4$ (Fluka, reagent grade) was dried under vacuum at 120 °C. Both PC and EC (Fluka, reagent grade) were purified by distillation under reduced pressure and separately weighted before mixing. EC was added to PC with a fixed molar ratio EC 46.5/PC 19. Stoichiometric amounts of $LiClO_4$ were added to the mixture and completely dissolved by heating the solutions at 60 °C. Concentrated solutions were prepared with ratios $N=0.069$, 0.22, 0.38, 0.47, 0.58, and 1.01.

Raman measurements on the various solutions have been performed using the 530.8 nm line of a Krypton laser for most of the spectra, but for the lowest concentrations ($N=0$ and $N=0.069$) where the 514.5 nm line of an Ar^+ ion laser has been employed. Some preliminary measurements have also been made by using the 488 nm Ar^+ laser line. A double Raman monochromator Jobin–Yvon (Ramanor HG2-S) equipped with holographic gratings (2000 lines/mm) was used to resolve the spectra and the scattered light was detected by a cooled photomultiplier (RCA-31034A-02) operating at -35 °C in photon-counting mode. The resolution of the spectra was typically of the order of $2-3\ cm^{-1}$. All the samples were sealed in cylindrical glass cuvettes. The spectra were collected always in the liquid state; for the partially crystallized compositions a previous heating treatment was performed at the temperature of about 80 °C some hour before the measurement, to allow a slow thermalization to room temperature. The same conditions of incident laser intensity, slit widths, monochromator speed and integration time were maintained to allow a better comparison of the spectra (see Results and Discussion).

^7Li NMR measurements were performed at 155.6 MHz on a Bruker AMX400 spectrometer ($B_0=9.4$ T), using a multinuclear, high-resolution 5 mm Bruker probe. Spin-lattice relaxation times (T_1) were extracted from the recovery profiles of the usual inversion recovery (IR) pulse sequence. The recovery behaviors were found to be exponential for all samples and over the entire temperature range. A 90° pulse of 5 μs and a recycle time of 20 s were used.

DSC measurements were performed on samples of about 20 mg under N_2 flow, using a DSC 910 unit (DuPont, USA) interfaced to a TA2000 thermal analysis system (TA Instruments, USA). The samples were encapsulated into aluminium pans, and cooled down to -150 °C using liquid N_2. The average cooling rate was estimated to be ~ 30 °C/min. The heating rate of the DSC runs was 10 °C/min.

Conductivity measurements were carried out using a modified Amel conductivity cell (platinum electrodes) and a Schlumberger 1260 impedance/gain-phase analyzer (frequency range, 1 Hz–400 kHz) over the temperature range 20–80 °C. The cell was calibrated using KCl standard solutions and its temperature was controlled by a thermostatic oil bath within ± 0.05 °C.

III. RESULTS AND DISCUSSION

A. The Raman information

The previous vibrational dynamics investigations on solutions or polymeric gels containing Li salts, and EC, PC or a mixture of both as solvents, have been performed via IR techniques[14–17] or Raman scattering.[5,6,11,17–19] In these studies, the most evident effect on the vibrational spectra of the solvents is the strong interaction of the ions with the ring breathing (ν_7) of EC molecule and ring bending mode (ν_8) of both the EC and PC species, which induces for the ''perturbed'' solvent molecules a frequency upshift of about $10\ cm^{-1}$ with respect to the unperturbed ones. The recent IR study[14] has been performed on solutions of $LiClO_4$ in pure EC, up to 30% of electrolyte content, while the Raman study,[5] also performed using pure EC as solvent, concerned relatively low (up to 1 M) electrolyte concentration. Raman investigations[18,19] made on PMMA polymeric gels embedded of PC/EC/$LiClO_4$ liquid solution up to 1 M showed the same effect on the ring vibrations of EC or PC molecules. In addition, comparison with other lithium salts having quite different anions demonstrated that Li^+ ions are chiefly involved in the interaction with the ring molecules of the solvent, whereas the changes of the spectral parameters for the solvent Raman bands are substantially independent from the anion.

The Raman spectra of the analyzed solutions are shown in Fig. 2 for the most interesting frequency range, including the ring modes and the perchlorate bands. To allow a direct quantitative comparison of the band intensities of the different spectra a proper normalization to an internal standard has to be performed. The total intensity of the bands assigned to –CH stretching (the integral of the experimental curve between $2800\ cm^{-1}$ and $3150\ cm^{-1}$, after straight line subtraction of the luminescence background) has been chosen as a standard. In fact, the intensity for a band at Raman shift x can be written as

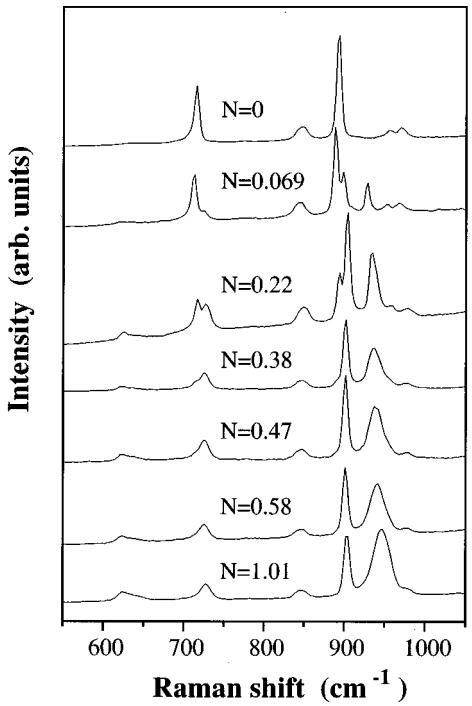

FIG. 2. Polarized (*VV*) Raman spectra between 550 and 1050 cm^{-1}, at different $LiClO_4$ concentrations in EC+PC solutions.

$$I = I_0 A S(x+x_0)\alpha(x_0)(x_0)^3(x+x_0)\frac{c(x_0)}{\nu}, \tag{1}$$

where I_0 and x_0 indicate intensity and wave number, respectively, of the excitation source, $S(x+x_0)$ is the response function of the gratings, A is a parameter depending on the alignment which can be considered constant during each measurement, the terms x_0^3 and $(x+x_0)$ give the usual off-resonance dependence on the excitation energy, $\alpha(x_0)$ is the real intensity of the band related to the Raman tensor and $c(x_0)/\nu$ is the number of the molecules vibrating at frequency x_0 in the scattering volume ν. By dividing the intensity of a generic band by the intensity of the –CH stretching of the same measurement, we obtain a normalized intensity,

$$I_N = \frac{S(x+x_0)}{S(x_{CH}+x_0)} \cdot \frac{(x+x_0)}{(x_{CH}+x_0)} \cdot \frac{\alpha(x_0)}{\alpha(CH)} \cdot \frac{c(x_0)}{c(CH)}, \tag{2}$$

where the first and second ratios have constant values for all the spectra obtained with the same excitation line (in any case, they change only of a few percent when the line is changed from 530.8 nm to 488 nm, and even less between 530.8 nm and 514.5 nm). The Raman intensity of –CH stretching can be reasonably assumed constant as a function of electrolyte concentration. In fact, a preliminary control insures that –CH stretching bands do not change appreciably their shape at all the electrolyte concentrations and, in principle, they involve localized group vibrations not directly concerned by the interaction with ionic species, and well distant in energy from the other bands. In addition, no appreciable dependence on the excitation wavelength has been found for the ratio $\alpha(x_0)/\alpha(CH)$ after some tests on different bands of solvent molecules, when ''green'' lines, i.e., 530.8 and 514.5 nm, were used. A significant variation could be observed only when the 488 nm line-excited spectra were analyzed. The ratio $c(x_0)/c(CH)$ contains the information we are searching for, on the population of the various molecular species, and it is expected to be constant when the total concentration of solvent molecules (unperturbed and Li^+-perturbed) is considered. Finally, the eventual changes of Raman tensor, measured by $\alpha(x_0)$, vs the electrolyte concentration, can be evaluated *a posteriori*, and result in any case small or not appreciable (see below).

Other choices are possible for the internal intensity standard: for instance, the perchlorate stretching band has been adopted in a previous Raman work on diluted solutions.[5] At high concentrations, however, the perchlorate stretching band overlaps with the solvent vibrations in such a way that eventual fit errors are no more independent. A plot of the total intensity of the perchlorate modes versus the ratio N is expected to increase linearly, if the molecular Raman tensors do not strongly depend on the electrolyte concentration and the instrumental factors affecting the measurement are properly accounted for. The above-made assumptions are corroborated by the observation of a quite linear trend (see Fig. 3, open squares) for the total Raman intensity normalized to the –CH stretching.

The main effects of the mobile ionic species on the vibrational dynamics of the solution concern the ring breathing mode ν_7 and the ring bending mode ν_8. The total Raman intensity for the bands ν_7 and ν_8, including both the perturbed and unperturbed components, appears nearly constant in all the concentration range analyzed, as expected if the assumptions of the Raman tensors independence from N are verified. The most interesting case of the ν_7 band can be seen in Fig. 4 (solid squares), where the intensity values are given by the sum of two Lorentzian components, representing the

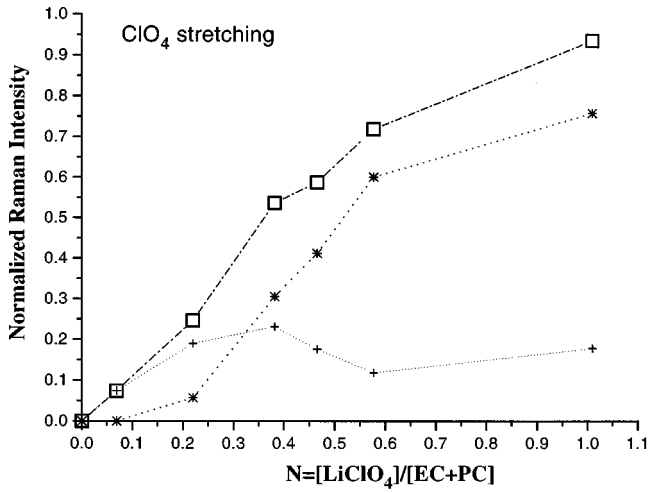

FIG. 3. Normalized total intensity of ClO_4^- symmetric stretching bands vs concentration of electrolyte (open squares), derived from a sum of two Lorentzian components. (a) Crosses represent the peak area of the free perchlorate ion stretching, at frequencies of 930–934 cm^{-1}; (b) asterisks represent the stretching intensity of associated ClO_4^- ions, having peak frequencies between 939 and 944 cm^{-1}. The normalization is always made with respect to the total area of CH_3 stretching bands.

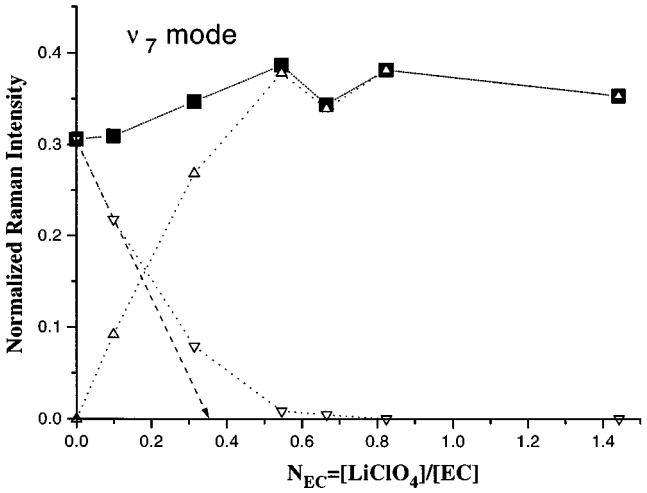

FIG. 4. Normalized intensity of the ν_7 band (solid squares), summing the perturbed (up-triangles) and unperturbed (down-triangles) components, as a function of the electrolyte concentration. The concentration variable N_{EC} is used, instead of N. The dashed arrow indicate the N_{EC} intercept extrapolated from low concentrations. The estimated error is of the order of 5%.

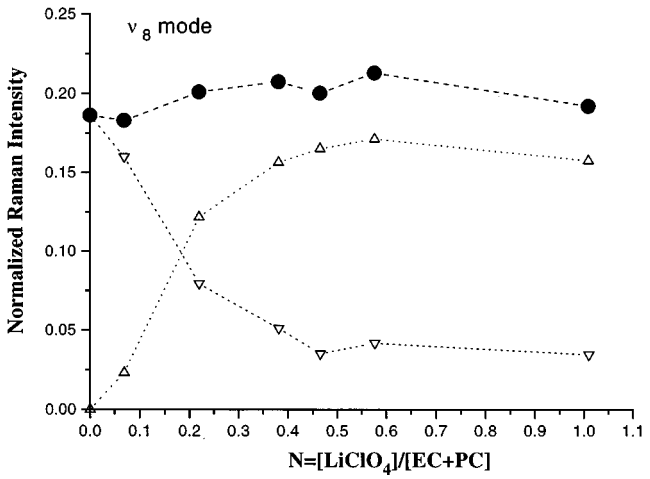

FIG. 5. Normalized intensity of the υ_8 band (solid circles), summing the perturbed (up-triangles), and unperturbed (down-triangles) components, as a function of the electrolyte concentration. The estimated error is of the order of 5%.

perturbed and unperturbed bands, which are also shown with different symbols (up- and down-triangles, respectively). Because the ν_7 band is present only in ethylene carbonate (EC) molecules, a modified concentration variable $N_{EC}=[LiClO_4]/[EC]$ must be used instead of N for such a band ($N_{EC}=N/0.7$).

The slight increase of the total normalized intensity for high N_{EC} values is consistent, in any case, with the slightly different Raman intensity per unit concentration $\alpha(x_0)$ of the perturbed ν_7 band; it has been found greater by a factor 1.09 with respect to the unperturbed ν_7 component for diluted solutions of pure EC.[5]

A quite similar behavior is shown by the ν_8 band, common to EC and PC. However, for such a ring bending mode occurring for the pure solvent at 715 cm^{-1} a more complex evolution seems to take place. In Fig. 5 the total intensity evolution (–CH normalized) is shown, together with the separate trends for the perturbed and unperturbed components, calculated by a Lorentzian fit. Also for this band a slight increase of the total intensity is observed at high N values, when the perturbed component dominates. The residual intensity in the frequency region of unperturbed ν_8 component can be due to the presence of other bands, observed even in the pure solvent sample, which affect the results of the fit. For instance, a ring bending mode was postulated in the low frequency side of this band by Durig and co-workers.[20]

The interaction with the ring modes can be described by dividing the solvent molecules into two populations; the unperturbed molecules and the perturbed ones. For these latter, the frequency of ν_7 mode is increased of about 10 cm^{-1} and that difference seems to be constant for all the concentration values where the two bands are observable. The bandwidths determination is more affected by fitting errors, but no great changes are observed for both the components, which have values between 5.5 and 6–6.5 cm^{-1}. This fact suggests that the ''perturbed'' and ''unperturbed'' states correspond to precise physical configurations, and not to intermediate states with continuously varying vibrational energy.

The most interesting information is given by the intensity ratio of the two components of ν_7 band; in the previous Raman work[5] it has been supposed that the value of Raman polarizability per unit concentration does not change versus the electrolyte content, so that an estimate of the solvation number, n, of Li^+ can be deduced from the intensity ratio of the two bands, and its value results between 4 and 5 for low electrolyte concentrations (corresponding to $N<0.069$). The hypothesis of the invariance for the Raman tensor can be maintained for all the examined compositions of the present study, because of the invariance of the normalized intensity for the sum of ν_7 components, as reported in Fig. 4. In addition, our data for low concentrations overlap the range discussed in Ref. 5, and give similar values for the intensity ratio of the two components, henceforth a similar value of n can be proposed. The extrapolation of that solvation number towards higher electrolyte concentrations is not verified by the present measurements.

Following the analysis of Ref. 5, an estimation of the solvation number can be deduced from the reciprocal value of the intercept with concentration axis of the curve fitting the decay of unperturbed ν_7 intensity. In fact, if we consider the normalized intensity of the unperturbed band, I_{un}

$$I_{un}=\frac{c_{un}}{c}\,\Gamma_{un}, \tag{3}$$

where c_{un} is the concentration of unperturbed solvent molecules, c the total concentration and Γ_{un} an absolute Raman intensity (also normalized by the –CH stretching intensity), from the basic relation,

$$\frac{M-n}{n}=\frac{c_{un}}{c-c_{un}}, \tag{4}$$

where n is the solvation number and $M=1/N=[\text{solvent}]/[\text{Li}]$, we obtain the following linear relation:

$$\Gamma_{un}-\Gamma_{un}nN=I_{un}. \tag{5}$$

In a plot of I_{un} vs N_{EC} (as in Fig. 4, down-triangles), the dependent variable $I_{un}=\Gamma_{un}$ can be defined as the normalized intensity in the pure solvent when $N_{EC}=0$. The solvation number n_{EC} is contained in the slope, and its value must be the reciprocal of N_{EC} at the intersection with the N_{EC} axis, when $I_{un}=0$.

As can be clearly seen in Fig. 4, the slope of this curve decreases with concentration and its intercept with concentration axis changes from $N_{EC}\cong=0.35$ to $N_{EC}\cong 0.7$. The first number corresponds to $n_{EC}\cong 2.8$, while the second corresponds to $n_{EC}\cong=1.4$. By assuming that EC or PC molecules enter the solvation shell in the same ratio of their relative concentration in the solvent, $n\cong 4$ is obtained at low concentrations and $n\cong 2$ is obtained at the critical concentration, which are the solvation numbers found in dilute solutions,[5] and that associated to the sandwich configuration postulated for high electrolyte contents,[11] respectively. On the basis of Raman data and their fitting analysis, it is hard to discriminate between a continuous slope change (decreasing exponential function) or a two-slopes behavior (two straight lines with the slope change occurring at about $N_{EC}\cong 0.35$). We can only say that the unperturbed component is barely detectable in the spectrum of $N_{EC}=0.7$, and disappears at higher concentrations. Thus, we can conclude that all the EC molecules are perturbed for $N_{EC}\geqslant 0.7$, and the value of n near this concentration is 2.

The perchlorate Raman modes display a linearly increasing total intensity vs the electrolyte concentration (but for $N=1.01$), as can be expected, but different evolutions can be described for two different components, representing different association states for the anions. For low concentrations, up to $N=0.069$, the perchlorate stretching occurs at 931 cm^{-1}, which is a well-accepted value for the free ion in diluted solution[17,21–23] and the band shape can be fitted by a single Lorentzian function with a small bandwidth (about 6 cm^{-1}). At higher concentrations, for instance at $N=0.22$, the band shape becomes asymmetric, and a reasonable fit needs (at least) two components, the first one at frequencies close to 930 cm^{-1}, and a second one centered at about 940–944 cm^{-1}, which corresponds to perchlorate anions reassociated with Li^+ cations, as it has been observed in other system containing perchlorate.[17,24] At increasing N the free-anion-component seems to remain constant or slightly decreasing in intensity, while the other one exhibits a strong increase above $N=0.22$ and becomes predominant (see Fig. 3, curves with crosses and asterisks, respectively). The separation of the different Lorentzians presents a large uncertainty at high concentrations, and quantitative estimate of the two ion populations from Raman intensities is meaningless. However, the qualitative difference between free-ion and pairing-affected stretching vibrations is quite evident, as confirmed also by the up-shift of the baricenter of the envelope band.

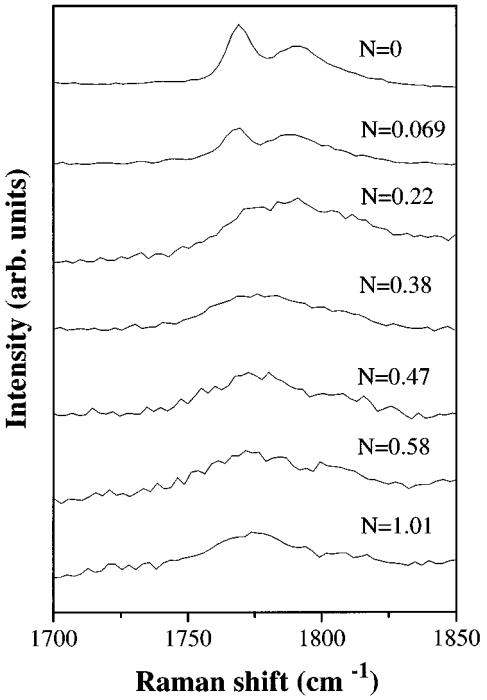

FIG. 6. Evolution of the Raman bands (Fermi doublet) in the carbonyl stretching region, vs $LiClO_4$ concentration.

In this apparent broadening and shift of the perchlorate band, a solvent band at 955 cm^{-1} merges with the perchlorate stretching distribution, as can be seen in Fig. 2. The next solvent band, occurring at 971 cm^{-1} in diluted solutions ($N=0$ and $N=0.069$), and assigned to a ν_6 (A_1) vibration,[25] upshifts to about 980 cm^{-1} in the more concentrated solutions. In addition, at high salt concentrations we observe with increasing intensity two bands between 620 and 640 cm^{-1}, which are assigned to other internal modes of perchlorate ions (the ν_4 band).

The interaction of Li^+ cations with the solvent molecules was expected to occur mainly close to the C=O carbonyl group because of the electronic charge distribution. However, the present Raman data show (see Fig. 6) that no special effect appears in the intensity distribution among the two C=O bands at 1770 and 1790 cm^{-1}, which are known to be sensitive to the external conditions of temperature, pressure and presence of polar molecules.[26] Similar results were obtained in Ref. 17.

The doublet appearing in the range 1750–1800 cm^{-1} is due to a Fermi resonance between the carbonyl stretching mode and the overtone of ν_7 vibration in EC molecules.[25,26] Only for pure solvent and low electrolyte concentration ($N=0.069$) the two components are well separated, while for any other concentration the components become broader and changes of spectral parameters are hard to be appreciated. This fact seems to indicate a rather continuous distribution of the interaction energy affecting the carbonyl bond, in a similar manner to the electrolyte-induced broadening of the ring bending mode ν_8 which involves the C=O group. On the contrary, the ring breathing mode ν_7 presents two

well-defined frequency distributions for the perturbed and unperturbed molecules. The comparison with the perturbation on the Fermi doublet induced by other molecules, for instance the neutral PMMA polymer chains,[18] suggests that no specific short-range interaction takes place between the Li^+ ions and the C=O bond. The observed effects on the carbonyl stretching bands for high values of N can be rather attributed to a general perturbation induced by the presence of foreign charged species.

In addition, no appreciable perturbation on the Fermi doublet appears at the lower concentrations, where a previous work and our present measurements indicate a solvation number of about 4. This fact conflicts with the existing pictures of Li^+ ions coordinated to the solvent molecules mainly via the C=O bond.[14] On the contrary, a configuration of the cations chiefly interacting with the ring oxygens of the solvent molecules and affecting the ring vibrations is more consistent with the Raman data at low N, also in agreement with the conclusions of Ref. 17. Such an interaction requires an eightfold coordination of the Li^+ ions, which has been reported in lithium complexes with ethers.[27]

B. The NMR information

Beside a description of the various configurations present in the solution, obtained by the Raman spectroscopy on a very short time scale ($\tau \sim 10^{-15}$ s), a complementary NMR investigation, working on much longer times of probe ($\tau > 10^{-6}$ s), can give additional information on the dynamics of these configurations.

Figure 7 shows the ^{7}Li spectra at 300 K for the solutions 0.22 (a), 0.58 (b), and 1.01 (c), and at 350 K for the solution 1.01 (d). The sample 0.22 displays two components; a broad one having a width of $\sim$400 Hz, and a narrow one at its upfield side. The situation is much more complex for the concentrated solutions, that display the growth of a complex structure in the spectrum. In addition, we note that the peak upfield side resembles a singularity. No appreciable chemical shift is found when increasing $LiClO_4$ content.

Figure 8 shows the ^{7}Li spin-lattice relaxation times of the examined solutions in the range 300–400 K. Broad T_1 minima are observed for the solutions 0.58 and 1.01 at $\sim$330 and $\sim$320 K, respectively. These minima may be related with the melting phenomena revealed by DSC, and describe the transition to the extreme motional narrowing regime, where the correlation time τ_c is of the order of the reciprocal Larmor frequency of the NMR experiment, ω_L^{-1}. The minimum of the most concentrated solution is shifted to lower temperature with respect to that of the solution 0.58, which indicates a higher mobility of the lithium ions. The solution 0.22 does not show the minimum in the studied temperature range.

The ^{7}Li NMR chemical shifts and line broadenings in nonaqueous solvents have been widely studied in early 1970s, both as far as concern pure solvated ions[28,29] and cryptates.[30] More recently, ^{13}C NMR has been used to investigate the effect of PC on the solvation shell of lithium ions in solutions with ether monomers.[31] However, all these works deal with diluted solutions, where the lithium concentration does not exceed 1 M.

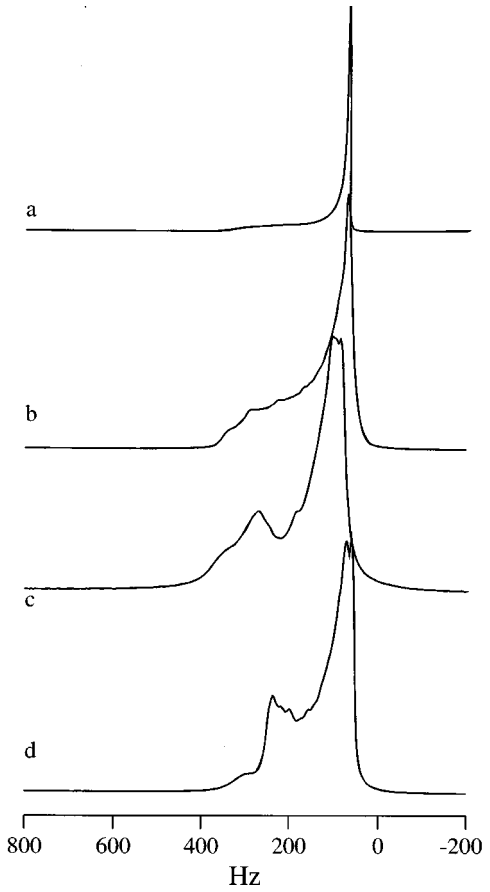

FIG. 7. ^{7}Li NMR spectra at 300 K for the solutions 0.22 (a), 0.58 (b), and 1.01 (c), and at 350 K for the solution 1.01 (d).

With any evidence, the spectra reported in Fig. 7 cannot be explained in terms of weakly interacting solutions, but require to consider the presence of (i) populations of lithium

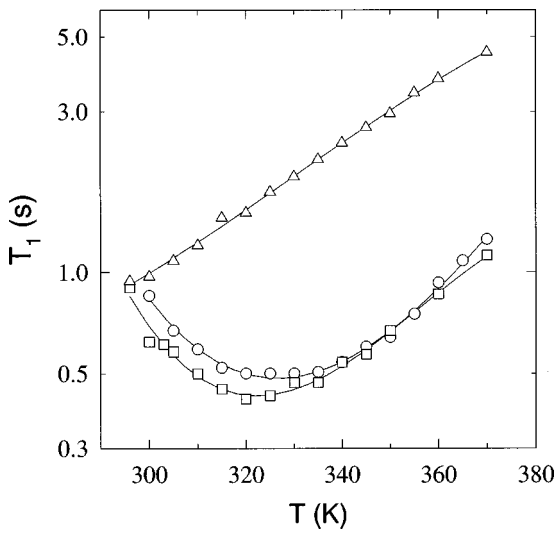

FIG. 8. ^{7}Li spin-lattice relaxation times in the range 300–400 K for the solutions 0.22 (triangles), 0.58 (circles), and 1.01 (squares).

ions having different mobilities, or (ii) one or more not fully averaged interactions. However, the former possibility is unlike, chiefly because of the very small chemical shift of lithium.[32] In addition, Fig. 7(d) shows that the structure is still present at 350 K, well above the T_1 minimum (see below), where the motional correlation times are not longer than 10^{-11} s. By itself, this fact rules out the anisotropies of chemical shift or magnetic susceptivity related to inhomogeneous broadening, and all other field-dependent interactions (like magnetic dipolar and electric quadrupolar) that are averaged by fast Brownian motion. As a matter of fact, we recall that ^{7}Li quadrupolar coupling constant, ν_Q, is of the order of 10^5 Hz.

On this basis, we can assign the complex structures displayed in Fig. 7 to a direct scalar spin–spin coupling interaction, not averaged by rapid motion, which is described by the following field-independent Hamiltonian[33]

$$\hbar H_{JJ}=\hbar\sum_{p<q} J_{pq}\mathbf{I}_p.\mathbf{I}_q+\sum_{q'} \hbar J_{q'}.\mathbf{I}'_q+\hbar H_l(I'), \tag{6}$$

where the I_n are the group of equivalent spins whose spectrum is under study, the I'_m are all the other spin of the molecule, and the last term is the part of the Hamiltonian that not depends on the spins I_n. The equivalence of the spins I_n is manifested through the fact that a single constant $J_{q'}$ describes the couplings of a spin I'_m with all the spins I_n.

Because of the shape of the spectra, this scalar interaction is supposed to arise between lithium and another ''abundant'' spin population, i.e., some protons of the solvent molecules. The task of understanding why the resulting spectrum is asymmetric is not a trivial one, and requires a quantum mechanical analysis of the spin states. If we suppose the interaction to hold between the complexed Li^+ and one proton of the solvent, we would expect to have a totally symmetric doublet. The asymmetries seen in Fig. 7 may be accounted for by considering that the width of a transition made by a spin $\mathbf{I}$ is related to the lifetimes of other spins $\mathbf{I}'$ coupled to it, which are determined by chemical exchange and/or magnetic or quadrupolar relaxation effects. A example in this sense is given by the ^{1}H spectrum of $-CH_3$ group in methyl alcohol,[34] where the much longer lifetime of the singlet state ($\mathbf{I}'_z=0$, $\mathbf{I}'=0$) with respect to the triplet one ($\mathbf{I}'_z=0$, $\mathbf{I}'=1$) determines an asymmetry of the two central lines. Consequently, the width of the narrow component is not related to the viscosity of the solution, but rather to the lifetime, τ_{cc}, of the complex formed by the Li^+ ions and by the solvent molecules. In order to justify the line shape of Fig. 7 the complex lifetime has to be longer than 100 ms.

A possibility to obtain a deeper understanding of this scalar interaction is to perform two-dimensional (^{7}Li,^{1}H) NMR experiments. We recall that our ^{13}C NMR data reported in Ref. 11 support the existence of a first ''critical'' point near a value $N\cong 0.2$, when the chemically-shifted peaks of the perturbed solvent molecules begin to be observable, that means a complex lifetime in the range of seconds. In fact, no anomalies has been found in the ^{13}C spectra of solutions with $N\leqslant 0.15$.

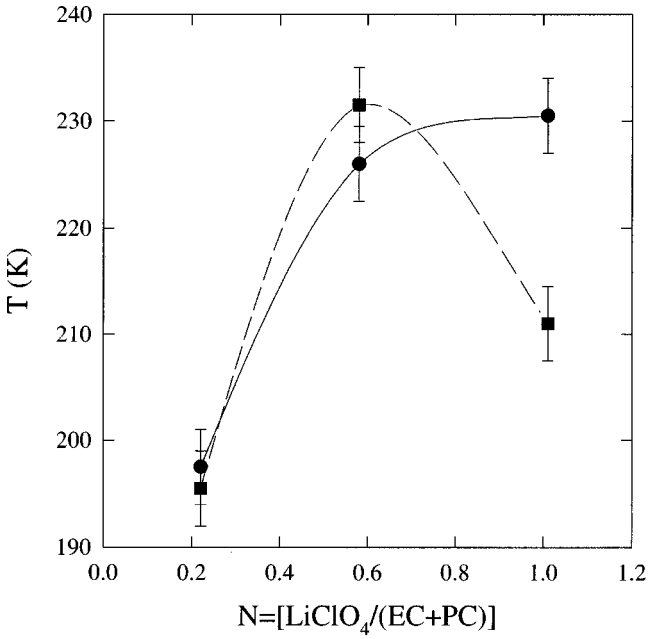

FIG. 9. Behavior of T_g (dark circles) and T_0 (dark squares) composition (see text).

C. Information from conductivity

In our previous paper[11] we showed that the conductivity displays a minimum vs salt concentration near $N\cong 0.5$. The compositions far from the critical concentration showed a well-defined Vogel–Tamman–Fulcher[13] behavior described by the equation

$$\sigma(T)=\sigma_0 A e^{-B/T-T_0} \tag{7}$$

all over the temperature range of the measurements (270–330 K). On the contrary, the compositions near the critical one followed VTF behavior just above $\sim$310 K, where the melting of a complex has been revealed by DSC. Below this temperature the curves assume a sigmoidal shape. Similar complex behaviors have been often observed in polymers, and may arise because the phase in which ionic conduction occurs is inhomogeneous, so that the thermal behaviour reflects phase melting and ionic flow among phases.[35]

The VTF equation was empirically derived to account for the viscosity behavior in supercooled liquids. In this framework, T_0 is just a reference temperature without any physical meaning. However, it is well known that the VTF relationship can be obtained in the frame of ''free volume'' model,[36] or also using the configuration entropy approach.[37] Within the former model, T_0 is defined as the equilibrium glass transition temperature where the free volume disappears, whereas in the latter one it is concerned with the vanishing of the configuration entropy of the system.

We fitted our data with Eq. (7), and showed that the conductivity is dominated by viscosity rather than by charge carriers concentration.[12] The best-fitting procedure treated T_0 as a adjustable parameter. In the case of compositions near the critical point, just the data taken at temperatures above the DSC melting endotherm were used for fitting. Figure 9

shows the behavior concentration of the glass transition temperature, T_g, as obtained by DSC, and the VTF parameter T_0, as extracted by conductivity data. T_g monotonously increases with salt concentration, whereas T_0 displays a maximum for $N=0.58$. In the limits of the uncertainty we may assume, the two parameters seem to coincide for the two lower compositions, while for $N=1.01$ T_0 falls ~ 20 K below T_g. This means that solutions $N=0.22$ and 0.58 behave like pure liquids in the temperature region where the best-fit was performed. The decoupling between T_0 and T_g observed for $N=1.01$ is likely due to the presence of undissociated crystalline $LiClO_4$, in agreement with our Raman result, and with the DSC data reported in Ref. 12.

IV. CONCLUSIONS

In a previous paper,[11] we have shown with Raman and ^{13}C NMR that a phase transition takes place at $N \cong 0.5$, where ''stable'' (in the second time scale) complexes are formed between a Li^+ and two solvent molecules, preferably an EC and a PC. Now, our overall spectroscopic and calorimetric findings allow us to sketch the following tentative model for the cations solvation in the pseudobinary system $LiClO_4$–(EC+PC):

(1) For $0 \leqslant N \leqslant 0.20$ the salt is completely dissociated and the cations are solvated by ~ 4 solvent molecules. The interactions likely occur between the Li^+ ions and the oxygens of the carbonate rings. The coordination lifetime is shorter than 1 ns. At room temperature, the solutions behave like a pure liquid both from DSC and NMR points of view.

(2) When the ratio N exceeds ~ 0.2, a part of the cations begins to interact with two solvent molecules. The complex lifetime is longer than tenth (or hundredth) milliseconds. Although the number of such complexes is still small, ^7Li NMR already reveals the existence of spin–spin coupling. The fraction of perturbed solvent molecules against salt content approaches a linear behaviour with an intercept corresponding to a solvation number $n \sim 2$.

(3) For N approaching 0.5, practically all the Li^+ ions are ''sandwiched'' between two solvent molecules. The existence of a crystalline complex which melts at $\sim 45\,^\circ C$ is witnessed both by conductivity and DSC data. Raman shows that all solvent molecules are complexed.

(4) For $N > 0.5$, finally, a partial reassociation of the salt takes place, as demonstrated by Raman spectroscopy and DSC.

[1] R. M. Fuoss and F. Accascina, *Electrolyte Conductance* (Interscience, New York, 1959).
[2] J. E. Desnoyers and C. Jolicoeur, *Comprehensive Treatise of Electrochemistry* (Plenum, New York, 1983), Vol. 5, Chaps. 1 and 2.
[3] J. C. Justice, *Comprehensive Treatise of Electrochemistry* (Plenum, New York, 1983), Vol. 5, Chap. 3.
[4] H. Farber and S. Petrucci, *The Chemical Physics of Solvation*, edited by R. D. Dogonadze *et al.* (Elsevier, Amsterdam, 1986), Part B, Chap. 8.
[5] S.-A. Hyodo and K. Okabayashi, Electrochim. Acta **34**, 1551 (1989).
[6] S.-A. Hyodo and K. Okabayashi, Electrochim. Acta **34**, 1557 (1989).
[7] M. Xu, P. Firman, S. Petrucci, and E. M. Eyring, J. Phys. Chem. **97**, 3968 (1993).
[8] P. E. Stallworth, J. Li, S. G. Greenbaum, F. Croce, S. Slane, and M. Salomon, Solid State Ionics **73**, 119 (1994).
[9] See, for example, B. Scrosati and R. J. Neat, *Applications of Electroactive Polymers*, edited by B. Scrosati (Chapman & Hall, London, 1993), Chap. 6.
[10] A. Zaban, E. Zinigrad, and D. Aurbach, J. Phys. Chem. **100**, 3089 (1996).
[11] E. Cazzanelli, P. Mustarelli, F. Benevelli, G. B. Appetecchi, and F. Croce, Solid State Ionics **86–88**, 379 (1996).
[12] F. Croce, G. B. Appetecchi, P. Mustarelli, C. Tomasi, E. Quartarone, and E. Cazzanelli, Electrochim. Acta (to be published).
[13] H. Vogel, Phys. Z. **22**, 645 (1922); G. Tamman and W. Hesse, Z. Anorg. Allg. Chem. **156**, 245 (1926); G. S. Fulcher, J. Am. Ceram. Soc. **8**, 339 (1925).
[14] Z. Wang, B. Huang, H. Huang, L. Chen, R. Xue, and F. Wang, Solid State Ionics **85**, 143 (1996).
[15] R. Frech and S. Chintapalli, Solid State Ionics **85**, 61 (1996).
[16] S. Chintapalli and R. Frech, Solid State Ionics **86–88**, 341 (1996).
[17] D. Battisti, G. A. Nazri, B. Klassen, and R. Aroca, J. Phys. Chem. **97**, 5826 (1993).
[18] E. Cazzanelli, G. Mariotto, F. Croce, G. B. Appetecchi, and B. Scrosati, Electrochim. Acta **40**, 2379 (1995).
[19] E. Cazzanelli, G. Mariotto, G. B. Appetecchi, and F. Croce, Ionics **2**, 81 (1996).
[20] J. R. Durig, G. L. Coulter, and D. W. Wertz, J. Mol. Spectrosc. **27**, 285 (1968).
[21] K. Kasatani and H. Sato, Chem. Lett. **1986**, 991.
[22] C. I. Ratcliffe and D. E. Irish, Can. J. Chem. **62**, 1134 (1984).
[23] K. Viras, J. H. Thatcher, C. H. Nicholas, and C. Booth, Solid State Ionics **68**, 49 (1994).
[24] S. Schantz, L. M. Torell, and J. R. Stevens, J. Appl. Phys. **64**, 2038 (1988); J. Chem. Phys. **94**, 6862 (1991).
[25] B. Fortunato, P. Mirone, and G. Fini, Spectrochim. Acta A **27**, 1917 (1971).
[26] W. Schindler, T. W. Zerda, and J. Jonas, J. Chem. Phys. **81**, 4306 (1984).
[27] U. Olsher, R. M. Izatt, J. S. Bradshaw, and N. K. Dalley, Chem. Rev. **91**, 137 (1991).
[28] Y. M. Cahen, P. H. Handy, E. T. Roach, and A. I. Popov, J. Phys. Chem. **79**, 80 (1975).
[29] H. G. Hertz, H. Weingärtner, and B. M. Rode, Ber. Bunsenges. Phys. Chem. **79**, 1190 (1975).
[30] Y. M. Cahen, J. L. Dye, and A. I. Popov, J. Phys. Chem. **79**, 1289 (1975).
[31] D. Fish and J. Smid, Electrochim. Acta **37**, 2043 (1992).
[32] *NMR and The Periodic Table*, edited by R. K. Harris and B. E. Mann (Academic, London, 1978).
[33] A. Abragam, *The Principles of Nuclear Magnetism* (Oxford University Press, Press, London 1961), Chap. XI.
[34] J. T. Arnold, Phys. Rev. **102**, 136 (1956).
[35] M. A. Ratner, *Polymer Electrolyte Review*, edited by J. R. MacCallum and C. A. Vincent (Elsevier, London, 1987), p. 173.
[36] M. H. Cohen and D. Turnbull, J. Chem. Phys. **31**, 1164 (1959).
[37] J. H. Gibbs and E. A. Di Marzio, J. Chem. Phys. **28**, 373 (1958).